Time-Stretched ADC Arrays

Bhushan Asuri, Yan Han, and Bahram Jalali

Abstract—This brief analyzes the performance of a new type of analog-to-digital converters (ADCs) architecture. The approach contemplates stretching the analog signal in time prior to digitization. Its benefits include an increase in the effective sampling rate and the input bandwidth, and a reduction in the sampling-jitter noise of the digitizer. It builds on the recent demonstration of high-speed analog-to-digial (A/D) conversion where a photonic preprocessor was used to successfully stretch an analog electrical signal before electronic digitization. The brief considers parallel time stretch ADC arrays capable of processing continuous time signals. In particular the effects of interchannel offset and gain mismatch, and clock skew are described and are contrasted with those in a conventional time-interleaved system. A mode of operation unique to this system is outlined wherein interchannel mismatch errors are entirely avoided at the expense of resolution bandwidth.

Index Terms—Analog-to-digital conversion, optical signal processing, time stretch.

Fig. 1. Conceptual block diagram for (a) single channel and (b) multichannel TSADC.

I. INTRODUCTION

Time interleaved analog-to-digital converter (ADC) architecture represents the most popular solution to digitization of high-speed analog signals. In such systems, the analog signal is sampled by a parallel array of M digitizers, which are sequentially clocked at a rate f_s/M, each, where f_s is the desired aggregate sampling rate. The main limitation of this approach is the mismatch between parallel channels. Offset, gain, and clock skew between different channels introduce spurs in the spectrum of the digitized signal limiting the performance of the ADC [1], [2].

Photonic time stretch preprocessing has been shown to be an effective method for increasing the sampling rate and the input bandwidth of electronic ADCs [3], [4]. The basic time stretched ADC (TSADC) concept is shown in Fig. 1. The high-speed signal is captured and slowed down in time before electronic digitization. For application to time-limited input signals, a single channel system shown in Fig. 1(a) suffices. On the other hand, if the input signal is continuous, a parallel system, shown in Fig. 1(b), must be employed.

Time stretch preprocessing increases the input bandwidth and sampling rate of the electronic digitizer by the stretch factor m. More importantly the time stretch system allows one to capture a high-speed time-limited signal with a single low-speed electronic ADC, hence, eliminating the channel mismatch problem. Jitter in the sampling clock introduces an amplitude error the power of which increases quadratically with the signal frequency. By reducing the signal frequency, time stretch preprocessing reduces such errors [3], [4].

Photonic techniques have been shown to be powerful tools for manipulating the time scale of electrical RF signals [3], [4]. Detailed description of the photonic time stretch technique and its implementation have been described elsewhere [3], [4] and are beyond the scope of this brief. Here, we provide a brief description of the technique to convey its pragmatism.
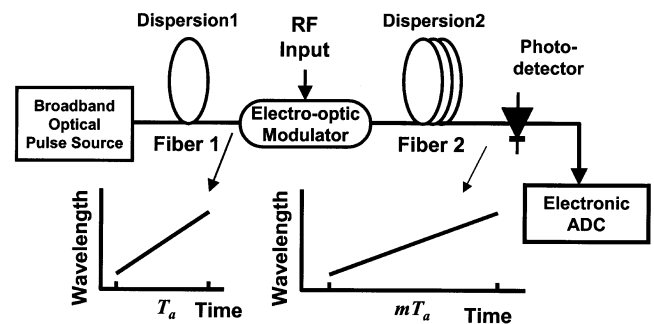
Fig. 2. Functional block diagram of the time-stretch preprocessor. The RF signal is modulated onto a linearly chirped optical carrier. The waveform is then (linearly) dispersed in the optical domain leading to temporal stretching of its envelope.

The block diagram for a photonic time-stretch preprocessor is shown in Fig. 2. A linearly chirped optical pulse is generated when a broadband (nearly transform-limited) optical pulse propagates in a optically dispersive device such as a spool of single mode optical fiber. The electrical signal modulates the intensity of this chirped optical carrier in an electro-optic modulator. The stretched envelope is produced after propagation through a second linearly dispersive fiber. After photodetection, the electrical signal represents the time-stretched version of the input RF waveform. Temporal-transformation is a two-step process. Step 1 is time to optical-wavelength mapping that occurs when the RF signal is modulated onto the linearly chirped optical carrier. Step 2 is the optical-wavelength to time mapping occurring in the second dispersive fiber. The stretched waveform is then digitized using an electronic ADC. Using this technique 130 Gsample/s digitization of time-limited RF signals has recently been demonstrated [4]. This has fueled interest in extending the time stretch A/D system to processing of continuous time signals.

It is intuitively apparent that a continuous-time signal can not be stretched using a single channel system. As shown in Fig. 1(b), for continuous time operation the input analog signal is segmented into M analog packets. Each packet is then stretched by a factor m before being digitized by an electronic digitizer. For an M channel system, the maximum stretch factor, $m_{\max} = M$. Fig. 3(a) and (b) shows block diagrams for two possible approaches to segmentation. In Fig. 3(a) the signal is split into M channels and then gated prior to the time-stretch
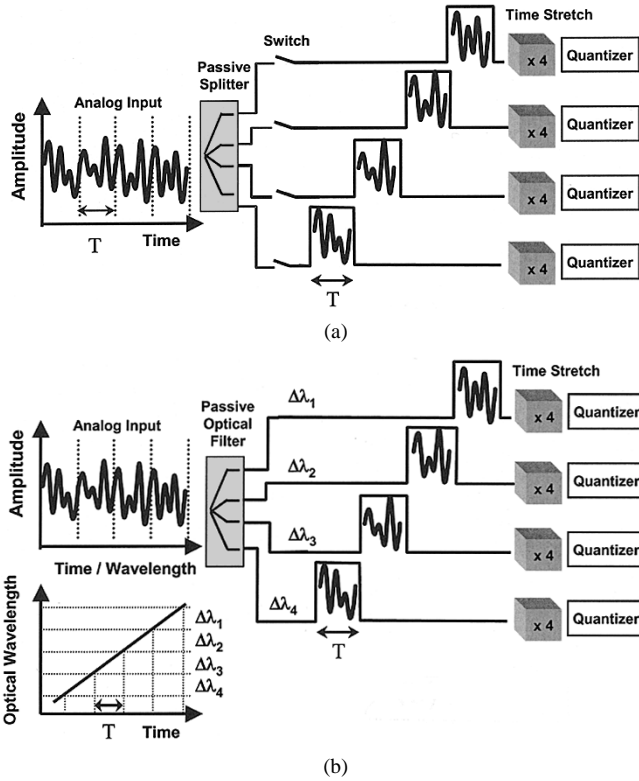
(a)

(b)

Fig. 3.　Two methods for segmentation. In Fig. 3(a), the signal is divided into four channels, which are sequentially gated using switches. In Fig. 3(b), the signal is modulated onto a linearly chirped optical carrier. A passive optical filter segments the optical spectrum. Owing to the time-to-wavelength mapping, this results in segmentation in the time domain.

block in each path. Segmentation is achieved by triggering the switches with a multiphase clock. In Fig. 3(b), the segmentation is performed in a completely passive method using time-to-wavelength mapping inherent in a chirped optical carrier. The RF signal is first modulated onto the chirped optical carrier, in a similar manner to that shown in Fig. 2. A passive optical filter then performs wavelength segmentation, which owing to the time-to-wavelength mapping, corresponds to the desired time segmentation. In the remainder of this brief, we refer to time stretched ADC arrays as "segment-interleaved" to be distinguished from the conventional time interleaved architecture which we will call the "sample-interleaved" system.

In this brief, we analyze the operation and performance of segment-interleaved time stretch ADC arrays. In particular we will elucidate and quantify the effects of interchannel offset, gain and clock skew on system performance.

II. MATHEMATICAL ANALYSIS

We study a segment-interleaved system with M parallel channels, analytically and by time-domain simulations. The segment in each channel is N samples wide. We start with offset mismatch and then study the effects of gain mismatch and clock skew. Interchannel offset mismatch introduces an error sequence that is periodic with a period $M \times N$. The error sequence in one period can be represented as follows: $[b_0, \ldots, b_0; b_1 \ldots, b_1; \ldots; b_{M-1}, \ldots, b_{M-1}]$. This sequence can be expressed as the circular convolution of the following two $M \times N$ sequences: $[b_0, 0, \ldots, 0; b_1, 0, \ldots, 0; \ldots; b_{M-1}, 0, \ldots 0] \circ [1, \ldots 1; 0, \ldots, 0]$ where $\circ$ stands for circular convolution. The discrete-Fourier transform (DFT) of the error
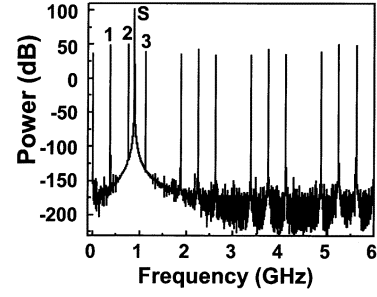

Fig. 4.　RF spectrum obtained from time-domain simulation for a four-channel segment-interleaved system with offset mismatch. The segments in each channel are four-samples wide. The offset errors create spurs at dc and harmonics of 375 MHz (6 GHz/16), with nulls at $k = 4, 8, 12, \ldots$ "S" denotes the signal and "1," "2," and "3" are the first three spurs.

sequence for discrete frequency parameter, $\omega = 2\pi k/M$, can be obtained by multiplying the DFT of the two sequences

$$F_k = \frac{1}{L} \left[\sum_{m=0}^{M-1} b_m \exp\left(-j\frac{2\pi km}{M}\right) \right]$$
$$\times \frac{\sin\frac{\pi k N}{L}}{\sin\frac{\pi k}{L}} \cdot \exp\left[-j\frac{\pi k(N-1)}{L}\right]. \quad (1)$$

In the above equation we have used $L = M \times N$. We can express the discrete time Fourier transform (DTFT) of the error using the DFT as follows:

$$Er(\omega) = \frac{2\pi}{T_s} \sum_{k=0}^{L-1} F_k \delta\left(\omega - \frac{k\omega_s}{L}\right). \quad (2)$$

This spectrum repeats itself at multiples of $\omega_s = 2\pi/T_s$, where T_s is the sampling period.

In Fig. 4, we present the spectrum obtained from the time domain simulation for a four-channel segment-interleaved system with offset mismatch. The segments in each channel are four-samples wide. The result is obtained by taking a 2^{17}-point DFT for a 887-MHz signal tone sampled at 6 GHz. The 4×4 offset error sequence used in the simulation is given by $b = [0 \cdots 0; 0.0066 \cdots 0.0066; -0.0186 \cdots -0.0186; 0.0077 \cdots 0.0077]$. As predicted by (1) and (2), the offset errors create spurs at dc and harmonics of $f_s/L = 375$ MHz, with nulls at $k = 4, 8, 12, \ldots$. The power in the highest spurs located at 375 MHz and 750 MHz relative to the signal power are -53 dB and -51 dB, respectively.

We now consider gain mismatch error. With the sequence $[b_0, \ldots, b_0; b_1 \ldots, b_1; \ldots; b_{M-1}, \ldots, b_{M-1}]$ representing gain mismatch error. The DTFT representing the output signal in the presence of gain mismatch can be described in terms of the analog spectrum of the signal $S^a(\omega)$ as follows:

$$Er(\omega) = \frac{2\pi}{T_s} \sum_{k=0}^{L-1} F_k \times S^a\left(\omega - \frac{k\omega_s}{L}\right).$$

The resulting spectrum for a sinusoidal input is given by

$$Er(\omega) = \frac{2\pi}{T_s} \sum_{k=0}^{L-1} F_k \times \delta\left(\omega - \omega_o - \frac{k\omega_s}{L}\right) \quad (3)$$

where ω_o is the signal frequency. In Fig. 5 we present the simulation results for a 4×4 system described above. The gain error sequence
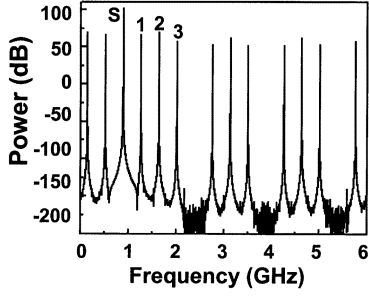
Fig. 5. RF spectrum obtained from time-domain simulation for a four-channel segment-interleaved system with gain mismatch. The gain mismatch creates spurs centered at 887 MHz spaced by harmonics of 375 MHz. "S" denotes the signal and "1," "2," and "3" are the first three spurs.
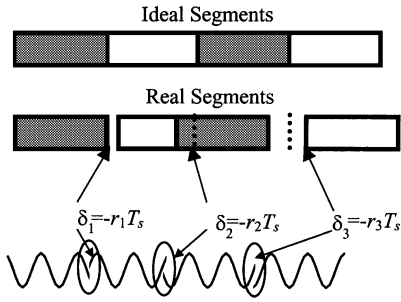

Fig. 6. Segmented system with clock skew. Each segment contains N samples. The segments are displaced from their ideal positions by $-r_m T_s$.

used in the simulation is given by $b = [1 \cdots 1; 1.03 \cdots 1.03; 0.94 \cdots 0.94; 1.07 \cdots 1.07]$. As predicted by (3), the gain mismatch creates spurs centered at 887 MHz spaced by harmonics of 375 MHz. The power in the spurs at 1262 MHz and 1637 MHz relative to the signal are -36 and -31 dB, respectively.

In order to understand the effect of clock skew, we consider the system shown in Fig. 6. Each segment contains N samples. The segments are displaced from their ideal positions by $-r_m T_s$. The sequence representing the samples captured in the system can be given as follows, $P = [s_{0,0} \cdots s_{0,N-1}; \ldots; s_{M-1,0} \cdots s_{M-1,N-1}; \ldots]$, where $s_{m,n}$ is the nth sample in the mth segment and can be represented as $s_{m,n} = [(m-1)NT_s + (n-1)T_s - r_m T_s]$.

By subsampling it at $M \times N \times T_s$ the sequence, P can be decomposed into the following $M \times N$ subsequences:

$$P_0 = [s_{0,0}(-r_0 T_s), \ s_{0,0}(-r_0 T_s + MNT_s), \ldots]$$
$$P_1 = [s_{0,1}(T_s - r_0 T_s), \ s_{0,1}(-r_0 T_s + MNT_s + T_s), \ldots]$$
$$P_N = [s_{1,0}(NT_s - r_1 T_s),$$
$$\quad\quad s_{1,0}(-r_1 T_s + MNT_s + NT_s), \ldots]$$
$$\vdots$$
$$P_{MN-1} = [s_{M-1,0}((MN-1)T_s - r_{M-1}T_s)$$
$$\quad\quad s_{M-1,0}(-r_{M-1}T_s + MNT_s$$
$$\quad\quad + (MN-1)T_s), \ldots].$$

We insert MN-1 zeros between each element of the subsampled sequences, P_j and shift them by j

$$\overline{P}_0 = [s_{0,0}(-r_0 T_s)(MN - 1 \ zeros),$$
$$\quad\quad s_{0,0}(-r_0 T_s + MNT_s), \ldots]$$
$$\overline{P}_N z^{-N} = [(N \ zeros), s_{1,0}(NT_s - r_1 T_s),$$
$$\quad\quad (MN - 1 \ zeros),$$
$$\quad\quad s_{1,0}(-r_1 T_s + MNT_s + NT_s), \ldots]$$
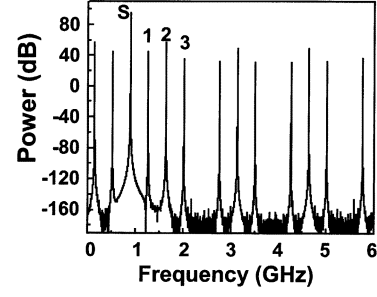

Fig. 7. RF spectrum obtained from time-domain simulation for a four-channel segment-interleaved system with clock skew. The skew error creates spurs centered at 887 MHz spaced by harmonics of 375 MHz. "S" denotes the signal and "1," "2," and "3" are the first three spurs.

$$\vdots$$
$$\overline{P}_{MN-1} z^{-(MN-1)} = [((M-1)N \ zeros),$$
$$\quad\quad s_{M-1,0}((MN-1)T_s - r_{M-1}T_s),$$
$$\quad\quad (MN - 1 \ zeros),$$
$$\quad\quad s_{M-1,0}(-r_{M-1}T_s + MNT_s$$
$$\quad\quad + (MN-1)T_s), \ldots].$$

In the previous equations, z is the unit delay operator. The sequence P can be reconstructed by adding the sequences $\overline{P}_j z^{-j}$. The DTFT representing the output signal in the presence of clock skew can be described in terms of the analog spectrum of the signal $S^a(\omega)$ as follows:

$$S(\omega) = \frac{1}{LT_s} \sum_{k=-\infty}^{\infty} \left(\sum_{m=0}^{M-1} \exp\left[-j\left(\omega - k\frac{2\pi}{LT_s}\right) r_m T_s\right] \right.$$
$$\left. \cdot \exp\left[-jkm\frac{2\pi}{M}\right] \right) S^a\left(\omega - k\frac{2\pi}{LT_s}\right)$$
$$\cdot \frac{\sin\frac{\pi k N}{L}}{\sin\frac{\pi k}{L}} \exp\left[-j\frac{\pi k(N-1)}{L}\right].$$

For a sinusoidal input, the spectrum can be written as follows:

$$S(\omega) = \frac{1}{T_s} \sum_{k=-\infty}^{\infty} F_k \delta\left(\omega - \omega_0 - \frac{k\omega_s}{L}\right) \tag{4}$$

$$F_k = \frac{1}{L}\left[\sum_{m=0}^{M-1} \exp(-j\omega_0 r_m T_s)\exp\left(-j\frac{2\pi k m}{M}\right)\right]$$
$$\cdot \frac{\sin\frac{\pi k N}{L}}{\sin\frac{\pi k}{L}} \cdot \exp\left[-j\frac{\pi k(N-1)}{L}\right]. \tag{5}$$

In Fig. 7, we present the simulation results for a 4×4 system described above. The skew error matrix is given by $r_m = [0.01 \cdots 0.01; -0.03 \cdots -0.03; 0.02 \cdots 0.02; -0.02 \cdots -0.02]$. The skew error creates spurs centered at 887 MHz spaced by harmonics of 375 MHz. From (4) and (5) the powers in the spurs at 1262 MHz and 1637 MHz relative to the signal are -50.4 and -38.3 dB, respectively.

III. DISCUSSION

According to the above results, channel mismatch errors in an interleaved time stretched ADC array (segment-interleaved array) are qualitatively similar to those in a sampled-interleaved system. Table I summarizes the results and compares them to the same for a sampled-interleaved system. In the case of offset error, the number of spurs that fall in a given bandwidth is N times higher in a segment-interleaved system compared to a sample interleaved system. While gain and clock skew introduce spurious sidebands in both systems, the sidebands are

TABLE I
EFFECT OF INTERCHANNEL MISMATCH ON A SEGMENT-INTERLEAVED ADC ARRAY COMPARED WITH THE SAME IN A TRADITIONAL SAMPLE-INTERLEAVED SYSTEM. f_s: AGGREGATE SAMPLING RATE; f_{in}: INPUT ANALOG FREQUENCY; M: NUMBER OF PARALLEL CHANNELS; N: NUMBER OF SAMPLES PER SEGMENT. A MAXIMUM STRETCH FACTOR, $m_{max} = M$ HAS BEEN ASSUMED

	Segment Interleaved	Sample Interleaved
Offset	Spurs at multiples of $f_s / N{\cdot}M$	Spurs at multiples of f_s / M
Gain	Spurs at multiples of $f_{in}/M \pm f_s/N{\cdot}M$	Spurs at multiples of $f_{in} \pm f_s/M$
Clock Skew	Spurs at multiples of $f_{in}/M \pm f_s/N{\cdot}M$	Spurs at multiples of $f_{in} \pm f_s/M$

closer to the carrier (by a factor N) in the segment-interleaved system. These results suggest that errors due to interchannel mismatches are more likely to fall in the signal band in segment-interleaved systems.

In both systems, mismatch errors are introduced when the analog signal is reconstructed, from samples in a sample-interleaved system, or from segments in a segment-interleaved system. If the reconstruction can be avoided, then mismatch errors can be prevented. While reconstruction is required in a sample-interleaved system, it may possibly be avoided in a segment-interleaved system. If the segment length is sufficiently long, each segment can provide the necessary spectral information. The minimum segment length is then determined by the required resolution bandwidth. In this mode of operation, subsequent segments simply update the captured signal spectrum at the segment arrival rate. Offset mismatch manifests itself as uncertainty in the dc component between each segment. Gain mismatch affects the signal amplitude resulting in an uncertainty in the absolute value of the power spectrum. However this does not affect the relative power of the spectral components, which is the quantity of interest in most applications. Clock (segment-to-segment timing) skew has no impact on the resulting spec-trum—it will introduce a time offset but no relative phase error between spectral components. Since the segment length might not always be an integer multiple of the RF signal period, the segmentation might introduce errors similar to the leakage errors in DFT. However the error can be minimized with windowing and/or sufficiently long segments.

In summary, we have analyzed parallel time stretch ADC arrays. This is a new ADC architecture where the signal is segmented and stretched in parallel channels prior to digitization by an array of ADCs. Its benefits include an increase in the effective sampling rate and the input bandwidth, and a reduction in the sampling-jitter noise of the ADC. A photonic preprocessing technique capable of stretching fast electrical signals in time was described. It was shown that, upon reconstruction of the signal from individual time segments, interchannel offset, gain mismatch, and clock skew create errors that are qualitatively similar to those in conventional sample-interleaved systems. However, the new architecture offers the possibility of avoiding reconstruction altogether. This requires a segment length compatible with the desired resolution bandwidth.

REFERENCES

[1] W. C. Black and D. A. Hodges, "Time interleaved converter arrays," *IEEE J. Solid-State Circuits*, vol. SC-15, pp. 1022–1029, June 1980.
[2] Y. C. Jenq, "Digital spectra of nonuniformly sampled signals: Fundamentals and high-speed waveform digitizers," *IEEE Trans. Instrum. Meas.*, vol. 37, pp. 245–251, Apr. 1988.
[3] B. Jalali and F. Coppinger, "Data conversion using time manipulation," U.S. Patent 6 288 659, Sept. 11, 2001.
[4] A. S. Bhushan, P. V. Kelkar, B. Jalali, O. Boyraz, and M. Islam, "130GSa/s photonic analog-to-digital converter with time stretch preprocessor," *IEEE Photon. Technol. Lett.*, vol. 14, pp. 684–686, May 2002.